Frictional Convergence in a Decaying Vortex

Željka Fuchs[1]

Physics Department, Faculty of Science, University of Split, Split, Croatia; Physics Department and Geophysical Research Center, New Mexico Institute of Mining and Technology, Socorro, New Mexico, 87801 USA

Michael J. Herman and David J. Raymond

Physics Department and Geophysical Research Center, New Mexico Institute of Mining and Technology, Socorro, New Mexico, 87801 USA

[1] *Corresponding author address:* Željka Fuchs, Physics Department and Geophysical Research Center, New Mexico Institute of Mining and Technology, Socorro, New Mexico, 87801. E-mail: zeljka@kestrel.nmt.edu

Abstract

Cross-isobaric flow and Ekman pumping are investigated in a frictionally decaying vortex in a stratified atmosphere. Consistent with early work by Holton and others, it is found that the stratification limits the vertical penetration of the secondary circulation driven by friction, resulting in a more rapid spin down than is conventionally assumed. As a result the cross-isobaric flow and Ekman pumping are weaker and shallower than classical calculations would lead one to believe. The effect becomes stronger as the vortex becomes smaller. For vortices with horizontal scales of several hundred kilometers or less, the reduction is particularly pronounced, which raises questions about the efficacy of Ekman pumping in forcing convection in such vortices. The theory as it stands is limited to weak, linear vortices in which geostrophic balance holds approximately, though extensions of the analytical theory to stronger vortices may be possible.

1 Introduction

The idea that deep atmospheric convection may be forced by frictionally induced convergence and lifting in the atmospheric boundary layer (Ekman pumping) is a nearly uncontested staple of modern meteorological theory. Its modern application in idealized models appears to have originated in Charney and Eliassen (1949) and was used in the context of tropical meteorology by Charney and Eliassen (1964), Ooyama (1969), Holton et al. (1971), Charney (1971, 1973), Holton (1974), Wang (1988), Wang and Rui (1990), etc.

The simple, most widely used version of the model was challenged by Raymond and Herman (2012). In this version, Charney and Eliassen (1964) assumed that the secondary circulation arising from surface friction would extend through most or all of the troposphere, which means that the time constant for global spin down would be large compared to the time required to bring the boundary layer alone to a halt by friction. Holton (1965) pointed out a potential flaw in this argument, noting that the upward penetration depth of the secondary circulation is limited by the stratification of the atmosphere. In particular, for a horizontal scale L of the boundary layer flow, and hence of the secondary circulation, the vertical penetration depth of this circulation scales as $Z = fL/N$, where f is the Coriolis parameter and N is the Brunt-Väisälä frequency. Thus, for small to mesoscale disturbances in the tropics where $N/f \approx 300$ and $L \leq 300$ km, $Z \leq 1$ km, or much less than the depth of the troposphere, contrary to the assumption of Charney and Eliassen (1964). As a consequence, the time for spin down is small enough that the steady state idealization behind the usual Ekman pumping formula may be invalid. Raymond and Herman (2012) showed in a linearized, slab-symmetric model that this effect has major consequences for Ekman pumping in weak (i.e., linear) disturbances in the tropics with horizontal scales less than a few hundred kilometers.

Aside from possible non-linearity, two situations could invalidate the analysis of Raymond and Herman (2012). First, if the boundary layer flow is driven directly by some external mechanism, then it could be maintained as a steady flow in the face of the rapid spin down tendency produced by surface friction. An example of this is the case in which surface temperature gradients drive the boundary layer, as envisioned by Lindzen and Nigam (1987). Spatial variations in these gradients could then result in quasi-steady regions of convergence and divergence. Though friction plays an important role in determining the structure of such convergence patterns, it is not correct to ascribe the convergence to the friction per se, as the prime mover in this case is the pattern of surface temperature gradient.

The second possibility is that deep convection operates in a manner that can be idealized by an effective reduction in the Brunt-Väisälä frequency of the atmosphere. This would result in an increase in the penetration depth of the secondary circulation and a corresponding increase in its spin down time. Yano and Emanuel (1991), Emanuel et al. (1994), and Neelin and Yu (1994), among others, have postulated such a model, with a typical reduction in the Brunt-Väisälä frequency to approximately 30% of its dry value.

In their idealized model, Emanuel et al. (1994) assumed that convective inhibition is negligible over the tropical oceans. Actual measurements of convective inhibition over the ocean (e.g., Raymond et al., 2003) show convective inhibition values that are undoubtedly much less than they are over, say, the American high plains in the spring, but are nevertheless large enough to play a significant role in tropical convective dynamics. Furthermore, Raymond (1995) showed that surface heat and moisture fluxes were often more effective in reducing convective inhibition than lifting by the weak mesoscale vertical motions typical of oceanic regions. In such a situation, the initiation of deep convection by Ekman pumping may not occur at all, especially if the Ekman pumping is being weakened by the low-level spin down of the parent disturbance.

One might argue that the low-level convergence produced by a pre-existing region of convection is a result of Ekman pumping; if the convection is in a statistically steady state, then the steady relationship between friction, pressure gradient, and Coriolis force characteristic of Ekman pumping must exist. However, this diagnostic relationship does not prove that the Ekman pumping "caused" the convection. If Ekman pumping in the absence of convection is insufficient to get the convection started in the first place, then the origin of the convection must be sought elsewhere.

In modern numerical models of the atmosphere, no assumptions are made about the nature of frictionally-induced convergence, so the considerations raised here do not apply directly to the model results. However, they potentially apply to the interpretation of these results. Such interpretations may not matter to the producers of model forecasts, but they are important for understanding the physics of such models and attempts to make the models better. Thus, we believe that it is of practical as well as of theoretical importance to sort out issues of causality in the frictional atmospheric boundary layer.

As noted above, Raymond and Herman confined themselves to slab symmetry and to the frictional convergence in single spectral modes. The present paper extends this work to boundary layer flows in decaying, axisymmetric vortices. Axial symmetry is important because tropical cyclones are often idealized as being axisymmetric and frequently have Ekman pumping, i.e., cloud base mass fluxes matched to frictionally converged mass, invoked as a forcing mechanism for convection, e.g., Charney and Eliassen (1964), Ooyama (1964, 1969). Zhu et al. (2001) and Zehnder (2001) admit more complex convective closures in their minimal cyclone models, comparing pure Ekman pumping closures with schemes based on surface heat and moisture fluxes. Not surprisingly, significant differences in tropical cyclone development exist among their various alternatives.

Mathematical tractability still limits us to the linear case, which imposes significant restrictions on the direct comparison with tropical cyclone observations. Nevertheless, the results are interesting in their own right and can form the basis for future numerical calculations not limited by the constraints of linearization.

2 Model for spin down in axisymmetry

The hydrostatic, rotating Boussinesq equations linearized about a state of rest in cylindrical coordinates (r, θ, z) for a stably stratified atmosphere in axisymmetry $(\partial/\partial\theta = 0)$ are

$$\frac{\partial u}{\partial t} - fv = -\frac{\partial \pi}{\partial r} + F_r \quad (1)$$

$$\frac{\partial v}{\partial t} + fu = F_\theta \quad (2)$$

$$\frac{\partial \pi}{\partial z} - b = 0 \tag{3}$$

$$\frac{1}{r}\frac{\partial r u}{\partial r} + \frac{\partial w}{\partial z} = 0 \tag{4}$$

$$\frac{\partial b}{\partial t} + N^2 w = 0. \tag{5}$$

The velocity vector in the radial, azimuthal and vertical directions is $(u,\, v,\, w)$, the buoyancy perturbation is b, the kinematic pressure perturbation (the mean potential temperature times the Exner function) is π, f is the Coriolis parameter, and N is the Brunt-Väisälä frequency, assumed to be constant. Surface friction enters in the radial and azimuthal directions (F_r, F_θ) as a frictional force per unit mass, assumed to be linear in velocity and decreasing exponentially with height:

$$F_r = -\lambda u_s \exp(-\mu z) \tag{6}$$

$$F_\theta = -\lambda v_s \exp(-\mu z). \tag{7}$$

The vector $(u_s,\, v_s)$ is the surface wind, $\lambda = \mu C_D U_0$ is the inverse of the spin down time scale, where $C_D \approx 10^{-3}$ is the drag coefficient, U_0 is a characteristic velocity, and $\mu^{-1} = h_\mu$ is the depth over which surface friction acts.

The system of equations (1)-(5) can be combined into a differential equation for the time tendency of the kinematic pressure perturbation. Incorporating equations (6) and (7) leads to

$$\left(\frac{\partial^2}{\partial t^2}+f^2\right)\frac{\partial^2\pi_t}{\partial z^2}+N^2\frac{1}{r}\frac{\partial}{\partial r}\left[r\left(\frac{\partial\pi_t}{\partial r}\right)\right]= \\ -N^2\frac{1}{r}\frac{\partial}{\partial r}\left[r\lambda\left(fv_s+\frac{\partial u_s}{\partial t}\right)\exp(-\mu z)\right], \tag{8}$$

where $\pi_t = \partial\pi/\partial t$. To solve equation (8), we use the initial condition that $\pi(r,z) = \pi_G(r)$ at all levels and assume that the surface wind (u_s, v_s), surface pressure perturbation π_s, and time tendency of kinematic pressure perturbation π_t decay exponentially to zero with time according to $u_s, v_s, \pi_s, \pi_t \sim \exp(-\sigma t)$, as in Raymond and Herman (2012). Substituting the above mentioned time dependence into (8) results in

$$\frac{\partial^2\pi_t}{\partial z^2}+\frac{N^2}{\sigma^2+f^2}\frac{1}{r}\frac{\partial}{\partial r}\left(r\frac{\partial\pi_t}{\partial r}\right)= \\ -\frac{N^2}{\sigma^2+f^2}\frac{1}{r}\frac{\partial}{\partial r}\left[r\lambda\left(fv_s-\sigma u_s\right)\exp(-\mu z)\right]. \tag{9}$$

Evaluating equations (1)-(2) at the surface and solving them for surface winds u_s and v_s in terms of the surface pressure perturbation, we obtain:

$$u_s = -\frac{\lambda-\sigma}{f^2+(\lambda-\sigma)^2}\frac{\partial\pi_s}{\partial r} \tag{10}$$

$$v_s = \frac{f}{f^2+(\lambda-\sigma)^2}\frac{\partial\pi_s}{\partial r}. \tag{11}$$

Substituting these into (9), we find

$$\frac{\partial^2 \pi_t}{\partial z^2} + \frac{N^2}{\sigma^2 + f^2}\frac{1}{r}\frac{\partial}{\partial r}\left(r\frac{\partial \pi_t}{\partial r}\right) = \\ -\frac{N^2 \lambda G(\sigma)\exp(-\mu z)}{\sigma^2 + f^2}\frac{1}{r}\frac{\partial}{\partial r}\left(r\frac{\partial \pi_s}{\partial r}\right), \tag{12}$$

where

$$G(\sigma) = \frac{f^2 + \sigma(\lambda - \sigma)}{f^2 + (\lambda - \sigma)^2}. \tag{13}$$

The solution to this equation can be written as the sum of homogeneous π_{ht} and inhomogeneous π_{it} parts. For the homogeneous part we assume z dependence of the form $\pi_{ht} \propto \exp(-mz)$, which allows the equation for π_{ht} to be written in the form

$$\frac{\partial^2 \pi_{ht}}{\partial r^2} + \frac{1}{r}\frac{\partial \pi_{ht}}{\partial r} + \frac{(\sigma^2 + f^2)m^2}{N^2}\pi_{ht} = 0. \tag{14}$$

This is an unscaled form of Bessel's equation for the Bessel function of order zero. It has the solution

$$\pi_{ht} \propto J_0(kr) \tag{15}$$

where J_0 is the zeroth order Bessel function and

$$k = \frac{(\sigma^2 + f^2)^{1/2} m}{N} \tag{16}$$

is the radial wavenumber k. Note that σ will be determined later.

We write the full surface pressure distribution as a superposition of Bessel functions with different radial wavenumbers k, i.e., in the form of an inverse Hankel transform

$$\pi_s = \int_0^\infty D(k)\exp(-\sigma t)J_0(kr)kdk \tag{17}$$

with the expectation that this form will lead to an analytical solution to the full problem. The assumed time dependence $\exp(-\sigma t)$ is included explicitly. Note that σ in general is a function of k. The inhomogeneous part of the solution for π_t can therefore be written as an inverse Hankel transform as well,

$$\pi_{it} = \exp(-\mu z)\int_0^\infty C(k)\exp(-\sigma t)J_0(kr)kdk, \tag{18}$$

where C is proportional to D, but remains to be determined. The homogeneous part of the solution can then be written

$$\pi_{ht} = \int_0^\infty A(k)\exp(-mz-\sigma t)J_0(kr)kdk \tag{19}$$

where the inverse of the vertical penetration depth of secondary circulation m is obtained from (16):

$$m(k) = \frac{kN}{(\sigma^2+f^2)^{1/2}}. \tag{20}$$

Putting these together results in

$$\pi_t(r,z) = \int_0^\infty \left[C(k)\exp(-\mu z-\sigma t) + A(k)\exp(-mz-\sigma t)\right]J_0(kr)kdk. \tag{21}$$

We determine $C(k)$ by noting that

$$-\sigma\pi_s(r) = \pi_t(r,0), \tag{22}$$

which implies $-\sigma D(k) = C(k) + A(k)$, or

$$C = -A - \sigma D. \tag{23}$$

Hence,

$$\pi_t = \int_0^\infty [A(k)\exp(-mz) - (A(k) + \sigma D(k))\exp(-\mu z)]\exp(-\sigma t)J_0(kr)kdk. \tag{24}$$

Requiring zero buoyancy perturbation at the surface implies that

$$\left(\frac{\partial \pi_t}{\partial z}\right)_{z=0} = 0, \tag{25}$$

which yields $A(k) = -\sigma\mu D(k)/(\mu - m)$ and hence

$$\pi_t = \int_0^\infty \sigma D(k)\left[\frac{m\exp(-\mu z) - \mu\exp(-mz)}{\mu - m}\right]\exp(-\sigma t)J_0(kr)kdk. \tag{26}$$

Plugging the solution (26) into the differential equation (12) leads to a dispersion relation that is identical to the one found using slab-symmetry in RH12:

$$\sigma(k) = \frac{\lambda m G(\sigma)}{m + \mu}. \tag{27}$$

Finally, our solution for the kinematic pressure perturbation is obtained by integrating (26) in time and requiring that $\pi = \pi_s(r, 0) = \pi_G(r)$ at $t = 0$:

$$\pi = \int_0^\infty D(k)\left\{1 - \frac{m\exp(-\mu z) - \mu\exp(-mz)}{m - \mu}[1 - \exp(-\sigma t)]\right\}J_0(kr)kdk. \tag{28}$$

The initial state of the flow is therefore unsheared in the vertical with arbitrary radial structure. Setting $z = 0$ reduces this to the assumed surface pressure perturbation (17).

The buoyancy and vertical velocity are obtained from (3) and (5):

$$b = \int_0^\infty D(k) \frac{m\mu \left[\exp(-\mu z) - \exp(-mz)\right]}{m - \mu} \left[1 - \exp(-\sigma t)\right] J_0(kr) k dk \tag{29}$$

$$w = -\int_0^\infty D(k) \frac{\sigma m\mu \left[\exp(-\mu z) - \exp(-mz)\right]}{N^2 (m - \mu)} \exp(-\sigma t) J_0(kr) k dk. \tag{30}$$

Using the identity

$$\frac{1}{r} \frac{\partial r J_1(kr)}{\partial r} = k J_0(kr), \tag{31}$$

where J_1 is the Bessel function of order one, plus the mass continuity equation (4), we get an equation for the radial velocity component:

$$u = -\int_0^\infty D(k) \frac{\sigma m\mu \left[\mu \exp(-\mu z) - m \exp(-mz)\right]}{N^2 (m - \mu)} \exp(-\sigma t) J_1(kr) k dk. \tag{32}$$

The azimuthal velocity component is obtained from (1):

$$v = \frac{1}{f} \left[\lambda u_s \exp(-\mu z) + \frac{\partial u}{\partial t} + \frac{\partial \pi}{\partial r}\right], \tag{33}$$

where

$$\frac{\partial \pi}{\partial r} = -\int_0^\infty D(k) \left\{1 - \frac{m \exp(-\mu z) - \mu \exp(-mz)}{m - \mu} \left[1 - \exp(-\sigma t)\right]\right\} J_1(kr) k^2 dk, \tag{34}$$

and

$$\frac{\partial u}{\partial t} = \int_0^\infty D(k) \frac{\sigma^2 m\mu \left[\mu \exp(-\mu z) - m \exp(-mz)\right]}{N^2 \left(m-\mu\right)} \exp(-\sigma t) J_1(kr) dk. \tag{35}$$

Equation (33) can be written explicitly with help of (32), (34), and (35), but is not shown here due to its complexity.

3 Results and interpretation

We first analyze the surface winds derived in the previous section by invoking a simplified form of the dispersion relation. We then present computations of the radial structure of the radial and vertical winds for a specified radial distribution of surface pressure, given this simplified analysis.

3.1 Surface wind analysis

Our primary circulation is a rotating disturbance on which frictionally induced cross-isobaric flow acts, creating a secondary circulation. Friction is assumed to have an exponential decay in z: $F_{r,\theta} \propto \exp(-z/h_\mu)$ where we call $h_\mu = 1/\mu$ the surface friction depth. The characteristics of secondary circulation of interest in this analysis are the penetration depth of the secondary circulation $h_m = 1/m$ and the cross-isobaric wind u.

We simplify our system of equations by assuming a typical tropical boundary layer in a weakly disturbed region where winds are not too strong, i.e., $\lambda \ll f$. We note that $G(\sigma) \leq 1$ for spin down times σ^{-1} greater than the rotational time scale f^{-1}, which constrains $\sigma \leq \lambda$ for all positive real values of m.[2] Since $\lambda \ll f$, $G(\sigma) \approx 1$, resulting in $m(k) \approx Nk/f$ and $\sigma(k) \approx \lambda m/(m+\mu)$. The penetration depth of our secondary circulation is then $h_m \approx fL/N$,

[2]Solving the transcendental system (13), (20), and (27) reveals 6 distinct complex pairs of $\sigma(k)$ and $m(k)$. Only one pair is positive real with $\sigma(k) \leq \lambda$ for all values of k. The other pairs will be explored in a future work.

where L is the horizontal scale of the primary disturbance, $L = 1/k$. Thus, the secondary circulation depth increases in proportion to the horizontal scale of the disturbance.

We now compare the surface radial wind u_s predicted by our model with that for the steady state surface wind u_{ss} arising from classical Ekman pumping analysis. From (10) and (11) we infer that

$$u_s = -\left(\frac{\lambda - \sigma}{f}\right) v_s = -\frac{\lambda}{f}\left(\frac{\mu}{m + \mu}\right) v_s. \tag{36}$$

Neglecting the time derivative in (2) corresponds to setting $\sigma = 0$ in (36), so the steady state radial velocity is just

$$u_{ss} = -\left(\frac{\lambda}{f}\right) v_{ss} = -\frac{\lambda}{f^2 + \lambda^2}\frac{\partial \pi_s}{\partial r}, \tag{37}$$

where we have inferred the steady tangential surface wind v_{ss} by setting $\sigma = 0$ in (11):

$$v_{ss} = \frac{f}{f^2 + \lambda^2}\frac{\partial \pi_s}{\partial r}. \tag{38}$$

Taking the ratio of u_s to u_{ss} and employing the definitions of h_μ and h_m results in

$$u_s = \frac{h_m}{h_m + h_\mu} u_{ss}. \tag{39}$$

Since Ekman pumping is related to the cross-isobaric flow u, we conclude that

$$h_\mu \ll h_m \Rightarrow u_s \approx u_{ss} \Rightarrow \text{normal Ekman pumping} \tag{40}$$

$$h_\mu \gg h_m \Rightarrow u_s \ll u_{ss} \Rightarrow \text{suppressed Ekman pumping.} \tag{41}$$

Assuming that $h_m = fL/N$ with $f = 3\times10^{-5}$ s^{-1} and $N = 10^{-2}$ s^{-1} and taking a plausible tropical boundary layer value of $h_\mu = 600$ m, we find that $h_m \approx 300$ m for $L = 300$ km while

$h_m \approx 2900$ km for $L = 3000$ km. Thus at the smaller scale, $u_s \approx (1/3)u_{ss}$, while $u_s \approx u_{ss}$ for the larger scale. The steady state assumption for the cross-isobaric flow is therefore poor for scales smaller than several hundred kilometers.

3.2 Comparison with steady state case aloft

The steady state solutions for u and w aloft are relatively simple to compute from (2) and (4):

$$u_{steady} = u_{ss} \exp(-\mu z) \tag{42}$$

$$w_{steady} = -\frac{1}{\mu r}\frac{\partial r u_{ss}}{\partial r} \tag{43}$$

where $u_{ss}(r)$ is the steady surface radial wind defined above. However, the full solutions, as represented by (30) and (32) are non-local and require the specification of the surface pressure as a function of radius at the initial time $t = 0$, which we assume to have the form

$$\pi_s(r, 0) = \pi_G(r) = -\frac{p'}{\rho_0 \left[1 + (r/L)^2\right]} \tag{44}$$

where p' is the initial pressure deficit in physical units at the center of the vortex, ρ_0 is the air density, and L is the scaling radius scaling the pressure anomaly. Since $\pi_s = \pi_G$ at time $t = 0$, we invert (17) to obtain $D(k)$,

$$D(k) = \int_0^\infty \pi_G(r) J_0(kr) r dr, \tag{45}$$

from which the full $u(r, z, t)$ and $w(r, z, t)$ may be computed using (30) and (32). The associated integrals are computed numerically and the validity of these computations is verified by showing that the inverse Hankel transform of a function followed by the corresponding forward transform returns the original function to acceptable accuracy.

We select values of p' such that the maximum tangential wind at $t = 0$ and $z = 0$ equals 5 m s^{-1} for values of L shown in table 1. The maximum wind occurs at radius $r = r_{max} = L/3^{1/2}$ and we let $f = 3 \times 10^{-5}$ s^{-1}, $\lambda = 8.3 \times 10^{-6}$ s^{-1}, and $\rho_0 = 1.2$ kg m^{-3}. The same simplified assumptions about the forms of m and σ used above are employed here.

The third column in table 1 gives the ratio of radial Coriolis force fv to the centrifugal force v^2/r at the radius of maximum winds. A large value of this ratio means that geostrophic balance in the tangential flow (as assumed here) is a good approximation. As table 1 shows, geostrophic balance is a good approximation for the assumed maximum tangential wind of 5 m s^{-1} for L equal to 3000 km and 1000 km, marginal for 300 km, and poor for 100 km. The rightmost column shows the vertical scale h_m of the secondary circulation.

Figure 1 shows the actual radial surface winds for the decaying vortex and for the steady state approximation to these winds at time $t = 0$ for the cases listed in table 1. The actual radial winds are always less than the steady state approximation, with a significant deficit for the $L = 300$ km and $L = 100$ km cases. The radius of maximum radial inflow is also slightly greater for the actual winds in comparison to the steady state.

Figure 2 shows the vertical velocity profile in the secondary circulation at a radius of $r = L/10$ for the cases of table 1. The vertical velocity for the decaying vortex is significantly less than that arising from the steady state assumption particularly at levels above the penetration depth of the secondary circulation in the decaying case. Furthermore, the elevation of maximum upward motion decreases drastically as L decreases, reflecting the decrease in the penetration depth h_m.

4 Conclusions

The idea of Ekman pumping as a forcing mechanism for convection in the tropics is deeply embedded in the conceptual structure of tropical meteorology. The classical formulation of Ekman pumping assumes that the free tropospheric secondary circulation induced by surface friction has a time scale for spin down that is long compared to the spin down time of an isolated boundary layer. As a consequence of this, the time derivatives in the horizontal components of the momentum equation are ignored in the boundary layer, resulting in the classical expression for the cross-isobaric flow there and the associated vertical motion (Ekman pumping).

Holton (1965) showed that the vertical scale of the secondary circulation resulting from surface friction is limited by the stable stratification of the free troposphere, resulting in a free tropospheric spin down time much smaller than is normally assumed. This result implies that the momentum equation time derivatives cannot be ignored for a decaying vortex in the derivation of the cross-isobaric flow in the boundary layer. As a consequence, the classical Ekman pumping equation is incorrect and the vertical motion can actually be much smaller than estimated by classical theory.

Raymond and Herman (2012) put numbers to this result for a zonal jet structure periodic in the meridional direction and found that the actual cross-isobaric flow and secondary circulation are much shallower and weaker than the classical result for lateral jet scales of order several hundred kilometers or less. We extend this analysis to axisymmetric vortices with arbitrary radial structure, with similar consequences. A particularly interesting result illustrated here is that the vertical velocity is not only weaker than the classical Ekman pumping result, but it also exhibits a vertical scale that decreases with vortex size. This reflects the vertical scale of the secondary circulation.

These results are applicable, at least approximately, to weak tropical waves with radial scales of several hundred kilometers. They are technically limited to weak disturbances because of the linearization of the governing equations about a state of rest.

We point out that the current results would be modified in the direction of the classical Ekman pumping result if the disturbances of interest were coupled to moist convection in a manner that results in a reduction of the effective Brunt-Väisälä frequency. However, we argue in the introduction of this paper that such a model for the interaction of moist convection with the boundary layer flow is oversimplified. Our experience in the tropics argues for a much looser relationship between weak, large-scale vertical motion and moist convection, a relationship in which it is easier to separate cause from effect. If convection exists in association with frictionally modulated convergence in the boundary layer, then the convection cannot be thought of as being caused by this convergence unless the convergence would have existed initially in the absence of the convection. Unless this is so, the convergence is more likely to be a consequence of the convection rather than vice versa, and what is naively perceived as convection being forced by Ekman pumping in fact often is not.

This result is important, since it gives us a completely different conceptual picture of the forcing of moist convection in the tropics than exists in tropical meteorology today. An incorrect picture can lead us to causally incorrect choices in such things as the construction of cumulus parameterizations in large-scale atmospheric models.

A technical limitation of the current results and those of Raymond and Herman (2012) is that associated with the linearization of the governing equations. Overcoming this limitation is needed to extend the results to more realistic situations such as the behavior of convection in a developing tropical cyclone.

Another limitation is that the primary circulation (vortical or linear in structure) must actually spin down in the absence of deep convection. In other words, the circulation must not have an external energy source exclusive of deep convection that keeps frictional dissipation from spinning it down. An example in which such an energy source exists is a circulation driven by gradients in sea surface temperature. In such a circulation, boundary layer convergence modulated by friction may coexist with deep convection, but one cannot argue that friction causes this convection; the sea surface temperature gradient is the prime mover here.

Acknowledgments. This work was sponsored by National Science Foundation grant number ATM-1021049.

5 References

Charney, J., 1971: Tropical cyclogenesis and the formation of the intertropical convergence zone. *Lectures in Applied Mathematics*, **13**, American Mathematical Society, 355-368.

Charney, J., 1973: Movable CISK. *J. Atmos. Sci.,* **30,** 50-52.

Charney, J. G., and A. Eliassen, 1949: A numerical method for predicting the perturbations of the middle-latitude westerlies. *Tellus,* **1,** 38-54.

Charney, J. G. and A. Eliassen, 1964: On the growth of the hurricane depression. *J. Atmos. Sci.,* **21,** 68-75.

Emanuel, K. A., J. D. Neelin, and C. S. Bretherton, 1994: On large-scale circulations in convecting atmospheres. *Quart. J. Roy. Meteor. Soc.,* **120,** 1111-1143.

Holton, J. R., 1965: The influence of viscous boundary layers on transient motions in a stratified rotating fluid: Part I. *J. Atmos. Sci.,* **22,** 402-411.

Holton, J. R., J. M. Wallace, and J. A. Young, 1971: On boundary layer dynamics and the ITCZ. *J. Atmos. Sci.,* **28,** 275-280.

Holton, J. R., 1974: On the influence of boundary layer friction on mixed Rossby-gravity waves. *Tellus,* **27,** 107-115

Lindzen, R. S., and S. Nigam, 1987: On the role of sea surface temperature gradients in forcing low-level winds and convergence in the tropics. *J. Atmos. Sci.,* **44,** 2418-2436.

Neelin, J. D., and J.-Y. Yu, 1994: Modes of tropical variability under convective adjustment and the Madden-Julian oscillation. Part I: Analytical theory. *J. Atmos. Sci.,* **51,** 1876-1894.

Ooyama, K., 1964: A dynamical model for the study of tropical cyclone development. *Geofisica Internacional*, **4**, 187-198.

Ooyama, K., 1969: Numerical simulation of the life cycle of tropical cyclones. *J. Atmos. Sci.,* **26,** 3-40.

Raymond, D. J., 1995: Regulation of moist convection over the west Pacific warm pool. *J. Atmos. Sci.,* **52,** 3945-3959.

Raymond, D. J. and M. J. Herman, 2012: Frictional convergence, atmospheric convection, and causality. *Atmósfera*, **25**, 253-267.

Raymond, D. J., G. B. Raga, C. S. Bretherton, J. Molinari, C. López-Carrillo, and Ž. Fuchs, 2003: Convective forcing in the intertropical convergence zone of the eastern Pacific. *J. Atmos. Sci.,* **60,** 2064-2082.

Wang, B., 1988: Dynamics of tropical low-frequency waves: An analysis of the moist Kelvin wave. *J. Atmos. Sci.,* **45,** 2051-2065.

Wang, B., and H. Rui, 1990: Dynamics of the coupled moist Kelvin-Rossby wave on an equatorial beta plane. *J. Atmos. Sci.,* **47,** 397-413.

Yano, J.-I., and K. Emanuel, 1991: An improved model of the equatorial troposphere and its coupling with the stratosphere. *J. Atmos. Sci.,* **48,** 377-389.

Zehnder, J. A., 2001: A comparison of convergence- and surface-flux-based convective parameterizations with applications to tropical cyclogenesis. *J. Atmos. Sci.,* **58,** 283-301.

Zhu, H., R. K. Smith, and W. Ulrich, 2001: A minimal three-dimensional tropical cyclone model. *J. Atmos. Sci.,* **58,** 1924-1944.

L (km)	p' (hPa)	$(fv)/(v^2/r_{max})$	h_m (km)
3000	8.40	10.4	9.0
1000	2.80	3.46	3.0
300	0.84	1.04	0.9
100	0.28	0.35	0.3

Table 1: Parameters used in the numerical computations and the resulting value of h_m. L is the scaling radius for the initial pressure distribution. The pressure deficit at the center of the distribution p' is chosen so that the maximum tangential wind is 5 m s^{-1}. The next column shows the ratio of Coriolis force to centrifugal force at the radius of maximum wind $r = r_{max} = L/3^{1/2}$. The rightmost column is h_m, the vertical scale of the secondary circulation.

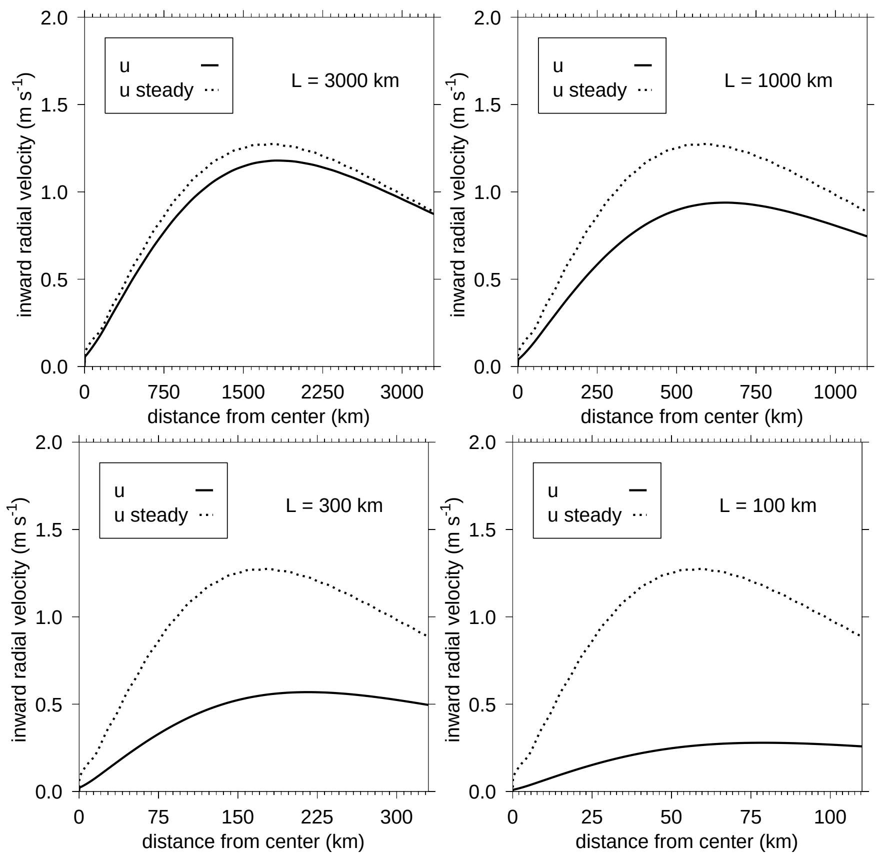

Figure 1: Surface radial velocity (solid) and corresponding steady state radial velocity (dotted) profiles for the initial radial distributions of perturbation pressure given in table 1. An inward velocity is taken as positive here.

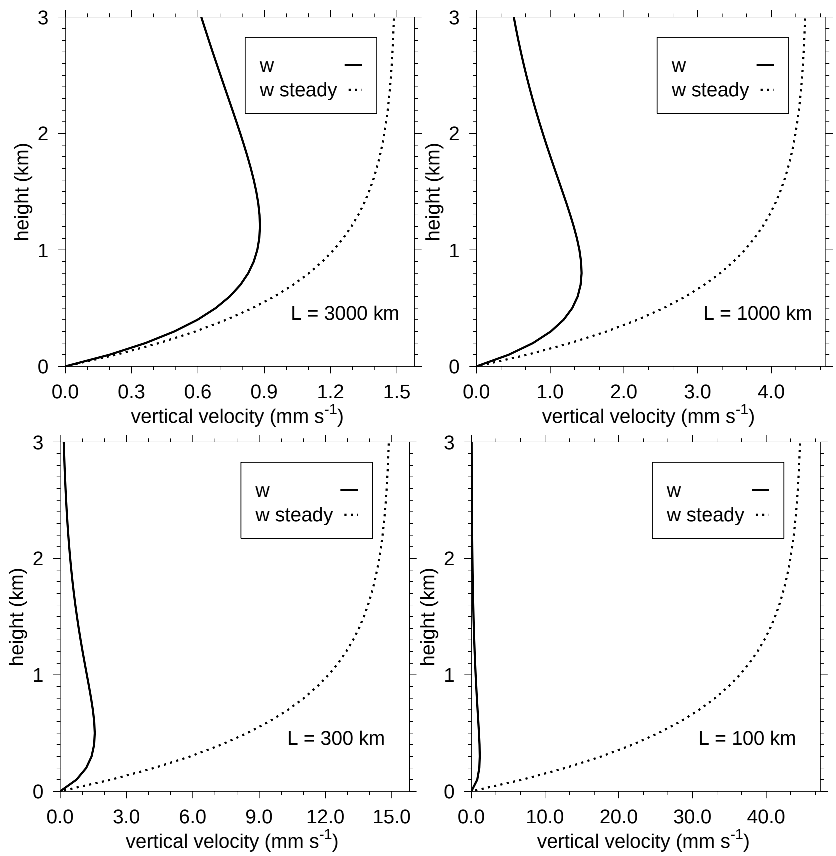

Figure 2: Vertical velocity (solid) and corresponding steady state vertical velocity (dotted) profiles at time $t = 0$ and radius $r = L/10$ corresponding to the cases illustrated in figure 1.